

12. MSL-2 ACCELEROMETER DATA RESULTS

Fred Henderson
Teledyne Brown Engineering

The Materials Science Laboratory-2 (MSL-2) mission flew the MSFC-developed Linear Triaxial Accelerometer (LTA) on the STS 61-C Shuttle mission launched January 21, 1986. Flight data have been analyzed to verify the quietness of the MSL carrier and to characterize the acceleration environment for future MSL users. The MSL was found to introduce no significant experiment acceleration; and the effects of crew treadmill exercise, Orbiter vernier engine firings, and other routine flight occurrences were established. The LTA was found to be well suited for measuring nominal to very quiet STS acceleration levels at frequencies below 50 Hz. Special processing was used to examine the low-frequency spectrum and to establish the effective rms amplitude associated with dominant frequencies.

The Materials Science Laboratory (MSL) was developed to provide a flexible cargo bay interface for experiments.

An objective of the MSL-2 Flight Accelerations Study was to evaluate Linear Triaxial Accelerometer (LTA) data obtained during the STS 61-C mission to determine the contribution, if any, of the MSL carrier to susceptible future experiments. Another primary objective was to quantify the acceleration environment for use by future MSL users (Figure 1).

The MSL-2 mission provided good data to satisfy these objectives, since LTA data were recorded continuously throughout most of

the six-day mission, and a wide variety of on-orbit circumstances were noted. Unlike Spacelab, there were periods when the entire crew slept, which enabled evaluation of a quiescent Shuttle. The effects of known crew-commanded disturbances were examined, and so was the behavior of the Shuttle during "quiet" periods of crew sleep.

- **VERIFY QUIETNESS OF MSL CARRIER SUBSYSTEMS**
- **QUANTIFY THE STS/MSL ACCELERATION ENVIRONMENT FOR MSL USERS**

FIGURE 1. OBJECTIVES

The STS 61-C cargo configuration, as depicted in Figure 2, consisted of one SATCOM satellite, which was deployed within hours of reaching orbit, several Get Away Special (GAS) canister experiments mounted on the GAS Bridge and on Hitchhiker-G1, and the MSL-2 payloads. The MSL was activated almost immediately upon start of on-orbit operations.

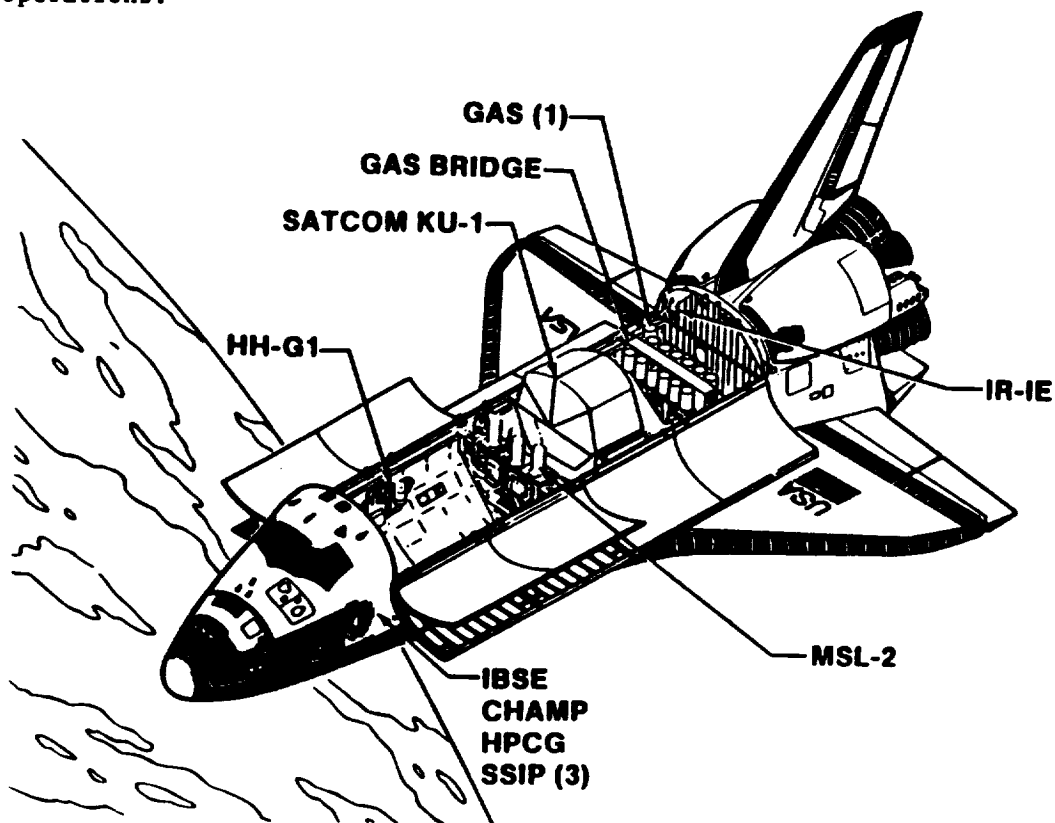


FIGURE 2. STS 61-C CARGO CONFIGURATION

The LTA is mounted on the aft side of the MSL carrier (Figure 3) with the signal junction box and instrumentation signal conditioners close to the OFT Freon pump. For this reason, the effect of pump operation was of some concern, although prior analysis had indicated that the 10,000-rpm rate of the pump would cause little carrier vibration.

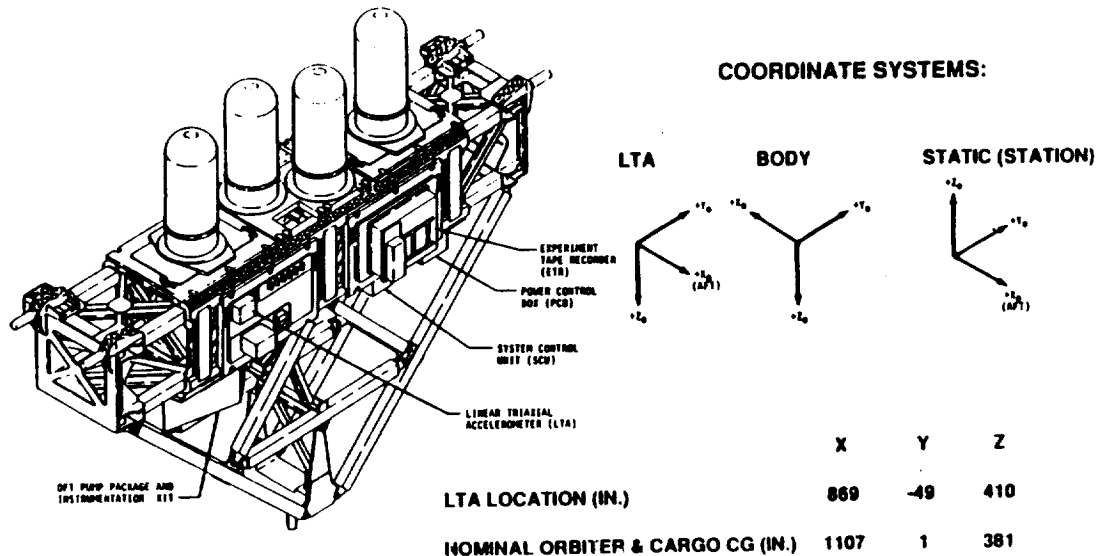


FIGURE 3. LTA ORIENTATION ON MSL

The location of the MSL is provided in static coordinates, as used to assign mechanical locations to the carrier. Orbiter body coordinates, LTA coordinates, and static coordinates all share the same respective axes but vary in declaration of the positive direction.

The LTA signal output range, resolution, accuracy, and frequency response are as specified in the accelerometer specification (Figure 4). The 125 sample/sec data acquisition rate for each channel was sufficient to determine frequencies well beyond the high filter corner frequency of 20 Hz.

| | |
|-----------------------|---------------|
| • RANGE: | ± 512 MICRO G |
| • RESOLUTION : | 1 MICRO G |
| • ACCURACY: | ± 5% |
| • FREQUENCY RESPONSE: | .01 TO 20 HZ |
| • SAMPLE RATE: | 125 SPS |

FIGURE 4. LTA CHARACTERISTICS

The lowpass filter of the LTA passes useful information well above the corner frequency of 20 Hz, as shown in the calculated plot (dashed line) and breadboard measured electrical response chart (solid line) of Figure 5. Discussions with the accelerometer vendor disclosed that the 20-Hz cutoff frequency was not the result of LTA mechanical limitations, but the addition of electronic anti-aliasing filters. The filter cutoff was based on an earlier intended application of the accelerometer, which required a slower sampling rate. Although attenuated, a significant portion of the input amplitude is passed through the electronic filter at frequencies less than the Nyquist frequency of 62 Hz.

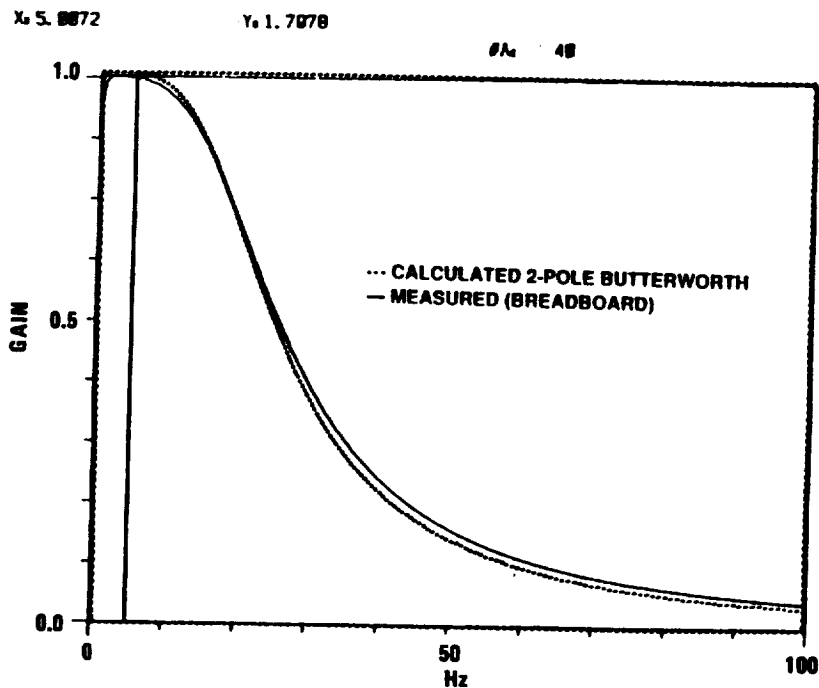


FIGURE 5. LTA LOWPASS FILTER RESPONSE

Including a mathematical model of the inverse lowpass filter function in the processing of LTA data enabled restoration of data as if the filter had not been present over the extended frequency range. This increased the susceptibility of the higher frequencies to random noise but enabled higher frequency spectral peaks to be observed. The effectiveness of the anti-aliasing filters on eliminating frequencies higher than 62 Hz was reduced, but no more so than the original anti-aliasing filter with respect to the original 20-Hz cutoff. The stages of the process used to effectively extend the frequency range is shown in the following discussion.

Data reduction techniques used to interpret LTA data began with the plotting of data from each axis on 2-hour plots (Figure 6). Although coarse, with the width of a line corresponding to over 2,000 data points, these plots were useful in showing periods of activity and quiet on a reasonably long time scale. Even so, 36 plots were required for each day of flight operation.

- TWO HOUR TIME HISTORIES
 - ESTABLISH PERIODS OF ACTIVITY
 - ESTIMATE DURATION OF QUIET PERIODS

- SHORT DURATION TIME HISTORIES (SECONDS)
 - SHOW STRUCTURE OF ACCELERATION HISTORY
 - CORRESPOND TO POWER SPECTRAL DENSITIES (PSD'S)

- POWER SPECTRAL DENSITY
 - AS RECORDED IN FLIGHT
 - WITH AND WITHOUT FILTER COMPENSATION
 - LOW FREQUENCY EXPANSION USING POINT AVERAGING
 - RMS AMPLITUDE AVERAGE OVER SPAN OF PSD
 - TOTAL AMPLITUDE
 - CONTRIBUTION NEAR DOMINANT FREQUENCY

- DISPLACEMENT HISTORY

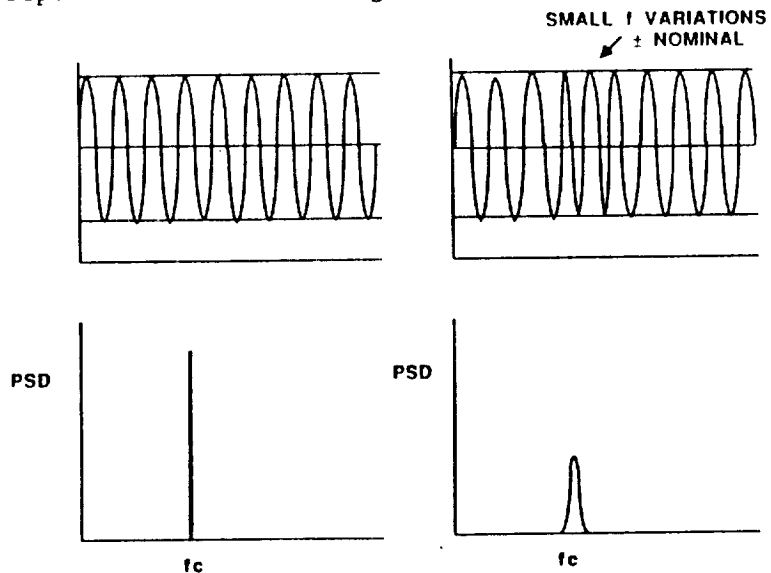
FIGURE 6. DATA REDUCTION TECHNIQUES

From these long-time-span charts and logs of mission activity, representative cases were chosen for further analysis. Representative plots spanning intervals from several seconds to minutes were examined to determine the nature of disturbances and to verify suitability for further treatment by application of Fast Fourier Transform (FFT) analysis.

For selected cases, power spectral densities (PSDs) were plotted, both from raw data and with filter compensation. Where low-frequency signals were present, plots of the low-frequency spectrum were expanded. An N point smoothing routine was added to permit measurement of very low frequencies approaching the 0.01-Hz low-frequency cutoff of the LTA while preserving the benefits of oversampling. Also, the ability to calculate in-band effective root mean square (rms) of PSD amplitudes around dominant frequencies was incorporated in the FFT program. In addition to in-band rms, rms calculations were also used to determine the total effective energy of data for all frequencies for comparison with the rms of time-history data. Agreement on total rms amplitude helped ensure validity of the process.

The PSD techniques, however, are limited in application to instances where conditions persisted over one to several seconds. While important in determining the nature of many disturbances, FFT analysis does not easily interpret irregular or occasional acceleration spikes that may also be damaging to low-g experiments. Consequently, a technique was developed to determine peak velocity and peak displacement resulting from LTA-sensed accelerations. Such calculations require that assumptions be made concerning a restoring system; otherwise, slight acceleration bias in the acceleration data will cause a gradual growth in derived velocity and quadratic growth in displacement. Insufficient data have been processed by this technique to publish results and so are not included here. Examples of some acceleration spikes, however, are included to illustrate the nature of LTA data.

One technique employed in LTA data analysis was the determination of effective rms amplitude of prominent PSD peaks. The reason for this is the possibility of slight frequency variations in LTA data causing a spreading of the PSD maximum amplitude. In such a case, as shown in Figure 7, the peak PSD amplitude of a pure frequency (as shown on the left) may be several times higher than the peak amplitude of a signal of identical amplitude (shown on the right) that exhibits slight variation in frequency. Computing the rms of PSD amplitudes surrounding the peak compensates for the frequency variation and yields a number proportional to the amplitude of the input signal. In each case shown, if the peak amplitude of the sinusoidal input were 10 mg, the rms amplitude reported would be 7.07 mg.



RMS OF FREQUENCY INTERVALS NEAR f_c WOULD SHOW EQUIVALENT
RMS AMPLITUDE

FIGURE 7. EXPLANATION OF IN-BAND RMS

Figure 8 shows the times when MSL equipment was active during the STS 61-C mission. Greenwich Mean Time (GMT), Mission Elapsed Time (MET), and MET hours are all shown on the scale across the top. The initial vertical line corresponds to launch on January 12, 1986, at 11

hours and 55 minutes. Other vertical lines are drawn at 24-hour intervals from the launch.

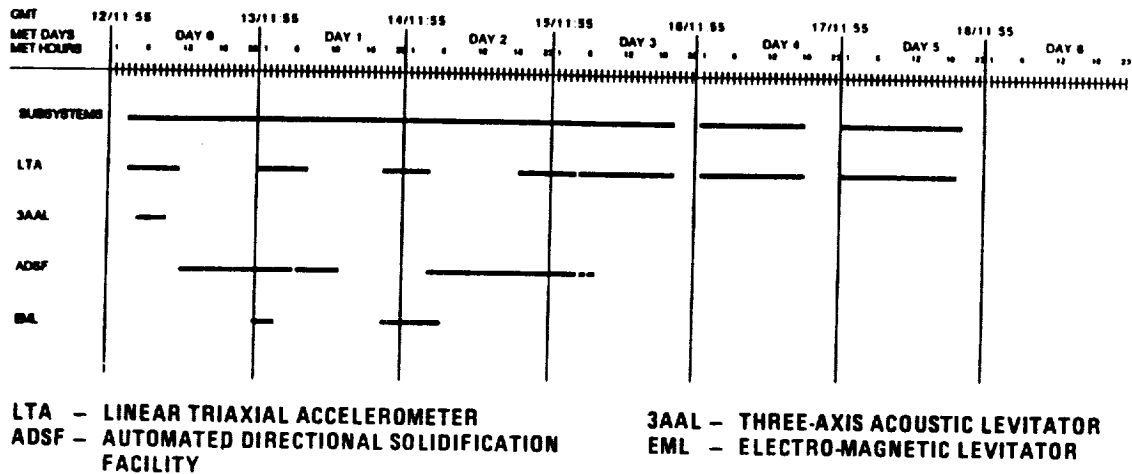


FIGURE 8. MISSION TIME PROFILE

As shown, the LTA acquired data for recording on the MSL Experiment Tape Recorder throughout most of the mission. MSL subsystems were activated soon after reaching orbit and remained on except for two periods later in the mission. These two periods of deactivation accompanied Shuttle landing preparations, which had to be deferred because of bad weather in the Shuttle landing area.

The notes in Figure 9 are shown to explain the representation of the acceleration data in the various time-history and PSD plots throughout this paper.

- REPRESENTATIVE AXIS CHOSEN FOR BREVITY
 - QUIETEST BACKGROUND PLOT USED TO SHOW NON-INFLUENCE
 - MOST ACTIVE AXIS USED TO SHOW SEVERITY
 - ALL AXES SHOWN IN MSL-2 FLIGHT REPORT, VOL. 2
- ACCELERATION AMPLITUDES ARE IN MILLI-G'S (MG'S)
- GMT DAYS 12-18 REFER TO CALENDER DAYS JAN. 12-18, 1988
- MAXIMUM VALUES NOTED ON PLOTS ARE IN ORDINATE UNITS (NOT RMS)
- RMS VALUES NOTED ON PLOTS REFER TO TOTAL DATA SET
- AMPLITUDES GREATER THAN LTA SATURATION LEVELS ARE VALID FOR FILTER COMPENSATED (ADJUSTED) PSD'S

FIGURE 9. DATE NOTES

A short time-history plot of LTA Y-axis data is shown in Figure 10. Full-scale amplitude is ± 0.512 mg beginning on January 18 at 2:48:00 and continuing for slightly over 4 sec. Also reported is the RMS amplitude of data and the mean amplitude.

As with subsequent figures, a representative axis has been chosen for brevity. Here the axis with the lowest background noise was chosen to show absence of pump interference. In other instances, the axis with the greatest amplitude is used to show severity of disturbances.

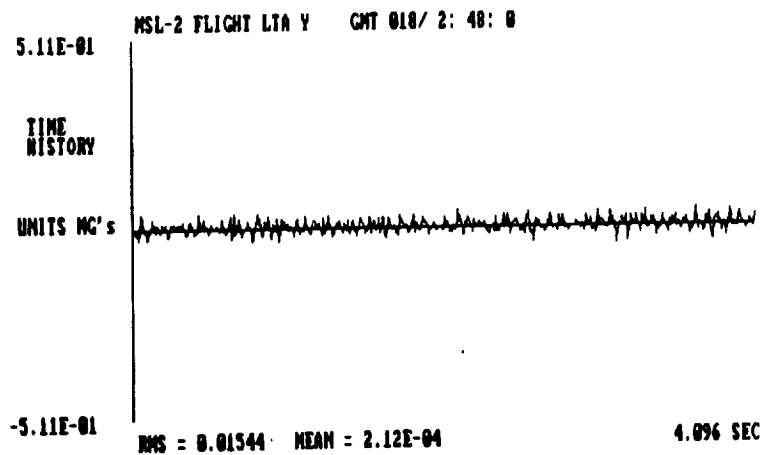


FIGURE 10. PUMP ON, 4-SEC TIME HISTORY

The PSD corresponding to the previous time-history (Figure 11) shows a moderate spectral peak around 13 Hz and a fairly random distribution elsewhere. Units are in milli-g's squared per hertz, and the maximum spectral intensity of 1.7×10^{-4} at 13.3 Hz is reported. The PSD-derived RMS amplitude of 0.01544 mg agrees with that derived from raw data samples on the previous chart. The FFT bandwidth of 0.2441 Hz is the width of each spectral band in the PSD.

The frequency domain data were treated by the inverse filter model and the PSD obtained as shown in Figure 12. As expected, the amplitude of high frequency contributors was amplified.

To verify repeatability, a second 4-sec sample of data was analyzed in the same way as the first (Figure 13), immediately following the first sample.

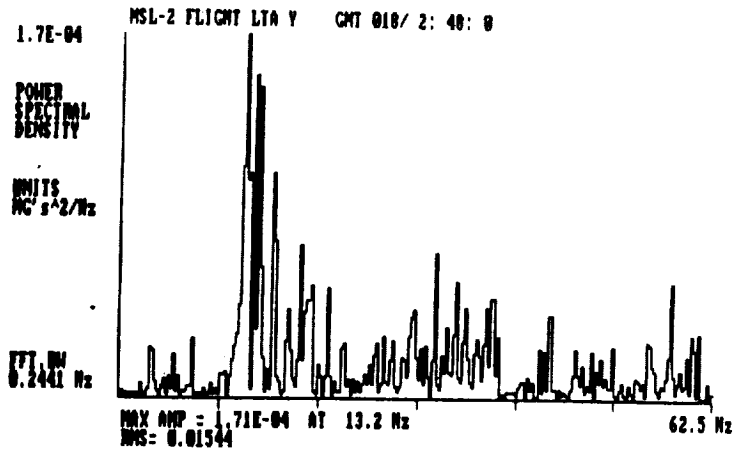


FIGURE 11. PUMP ON, 4-SEC PSD

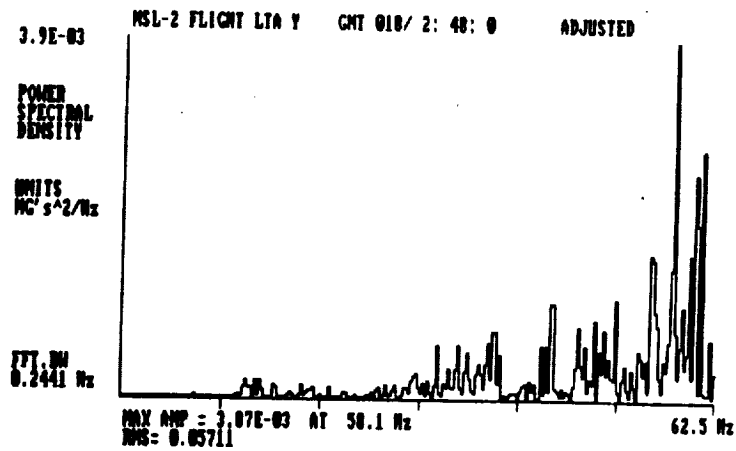


FIGURE 12. PUMP ON, 4-SEC PSD-ADJUSTED

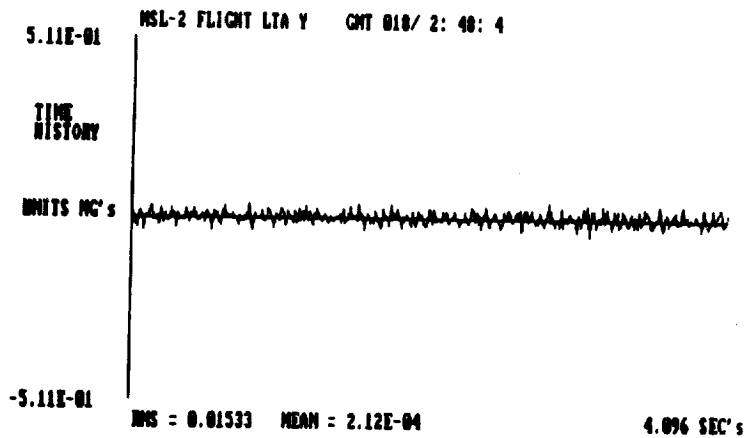


FIGURE 13. PUMP ON, 4-SEC TIME HISTORY

Again the filter-compensated PSD was taken to compare with the earlier sample (Figure 14). If peaks do not occur at the same frequency in each case, then the peak was most likely random or the situation measured changed from one 4-sec span to the next.

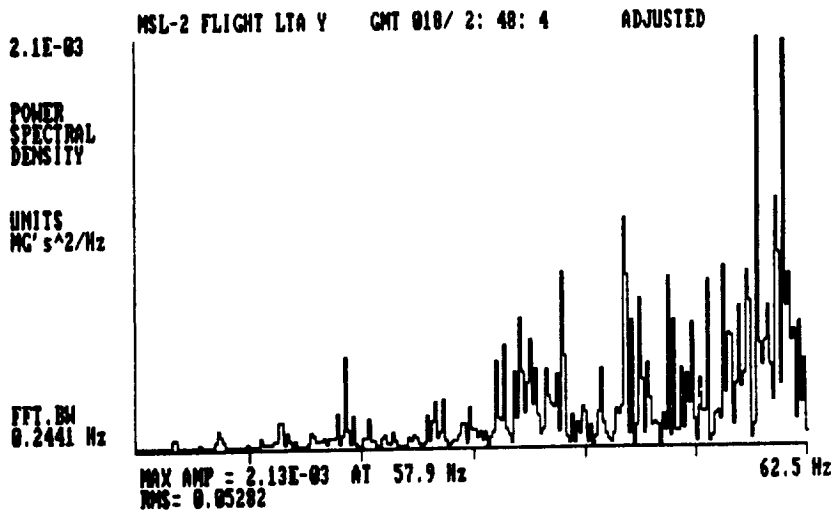


FIGURE 14. PUMP ON, ADDITIONAL 4-SEC PSD, ADJUSTED

If the sample is considered representative after comparison, then the composite time history with filter adjustment is obtained from the inverse FFT (Figure 15). This effectively reproduces the LTA signal as it was before the 20-Hz lowpass filter. It is possible to accurately report amplitudes greater than the 0.5-mg normal peak input of the LTA.

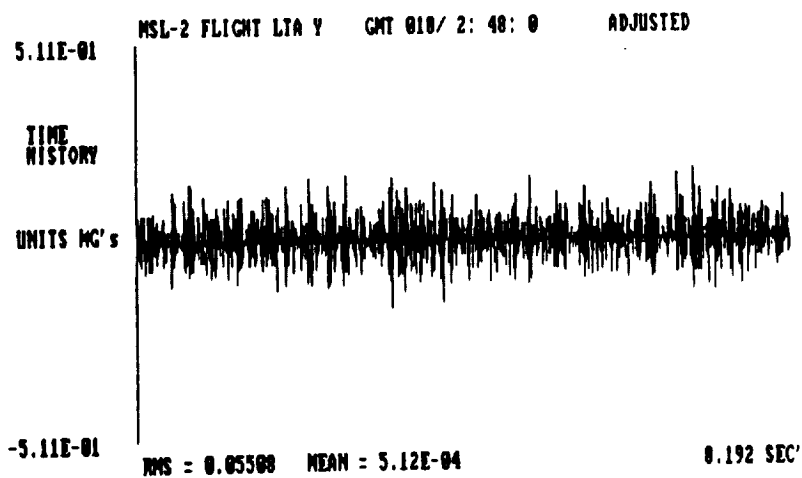


FIGURE 15. PUMP ON, COMPOSITE 8-SEC TIME HISTORY, ADJUSTED

The composite PSD obtained with filter compensation shows a probable spectral spike at 57.9 Hz (Figure 16). Since there is a possibility of some error being introduced by the filter-compensation amplification, both the adjusted and unadjusted 8-sec versions will appear in the flight report. All filter-compensated PSDs and time-history plots are denoted as "adjusted."

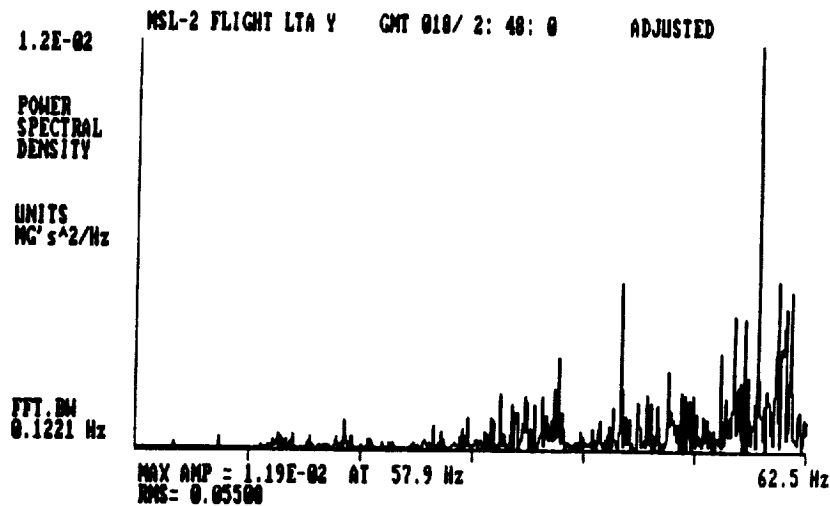


FIGURE 16. PUMP ON, COMPOSITE 8-SEC PSD, ADJUSTED

The low-frequency portion of the PSD is amplified (Figure 17) to show frequencies potentially more damaging to many experiments than the high-frequency spectra. If there is evidence of energy in the lower frequencies, the special processing technique is used to discern frequencies as low as 0.01 Hz by the application of a much longer time span of data.

The identical process, to the one performed for the pump-on case was repeated for the pump-off case shown in Figure 18. The adjusted time history appears much the same as that for the pump-on case.

The adjusted PSD of the pump off case (Figure 19) showed only slight variation from the pump-on case shown earlier. In fact, the rms value is slightly reduced.

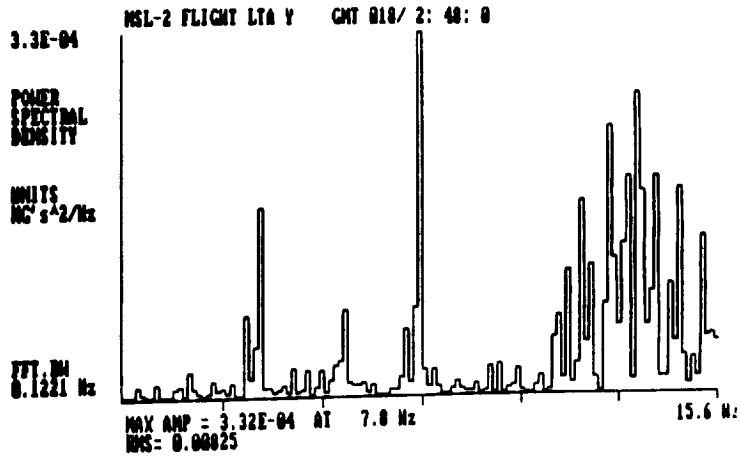


FIGURE 17. PUMP ON, LOW-FREQUENCY PSD

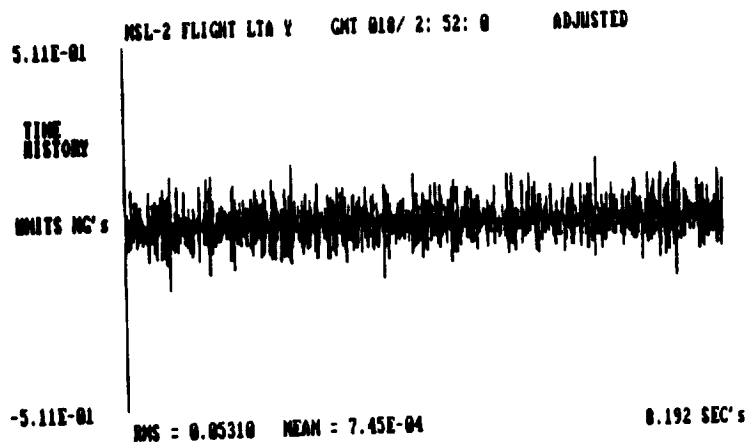


FIGURE 18. PUMP OFF, ADJUSTED TIME HISTORY

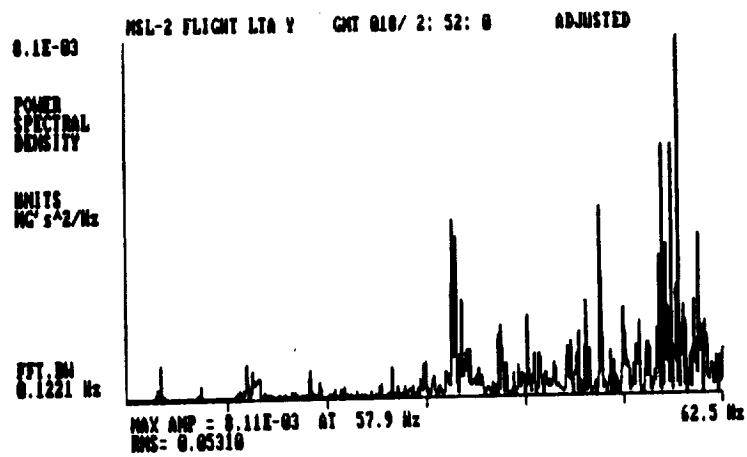


FIGURE 19. PUMP OFF, ADJUSTED PSD

As for the broad-frequency PSD, the low-frequency PSD shows little change with the pump off (Figure 20). From a comparison of data from all three LTA axes, it was concluded that operation of the Freon pump added little to the vibrations already present on the Shuttle.

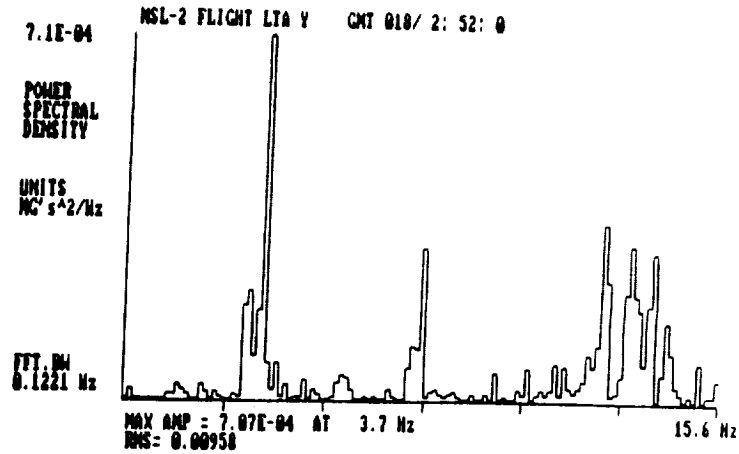


FIGURE 20. PUMP OFF, LOW-FREQUENCY PSD

As an added precaution, a PSD was taken from flight data with the LTA off to examine the possible presence of EMI or data system effects (Figure 21). This PSD was taken from flight data after the MSL System Control Unit, Freon pump, Experiment Tape Recorder, and Power Control Box had been activated but before the LTA was on. Had EMI been present on the data lines between the LTA and the MSL data acquisition system, it would be observable at this time. This PSD agrees with ground data that show RMS noise less than 0.1% for MSL measurements.

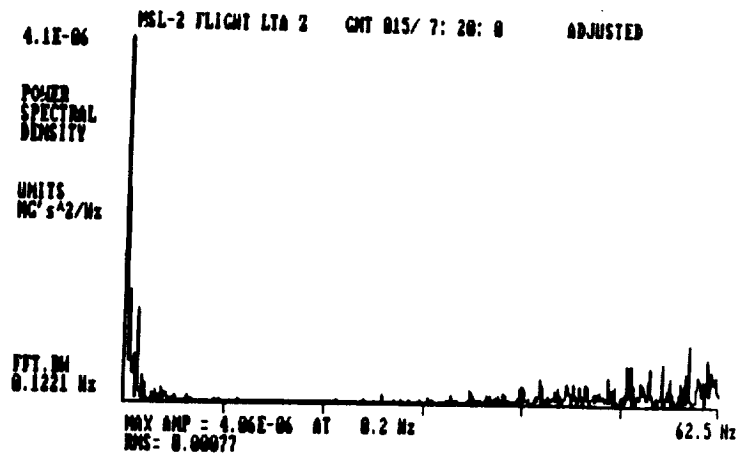


FIGURE 21. LTA OFF CASE

By contrast, data acquired during a crew exercise period using the treadmill show severe acceleration (Figure 22). It is difficult to estimate the true amplitude of the peaks because of saturation beyond ± 0.5 mg.

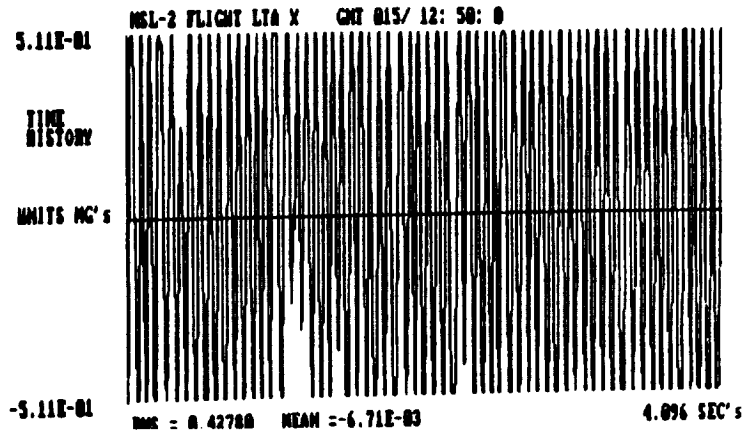


FIGURE 22. TREADMILL EXERCISE CASE, TIME HISTORY

As evident by the sinusoidal character of the time history, the PSD shows a predominant frequency (Figure 23). The greatest spectral amplitude is at 15.4 Hz. This and the energy in the frequencies within 3 Hz account for most of the 0.675-mg rms amplitude reported.

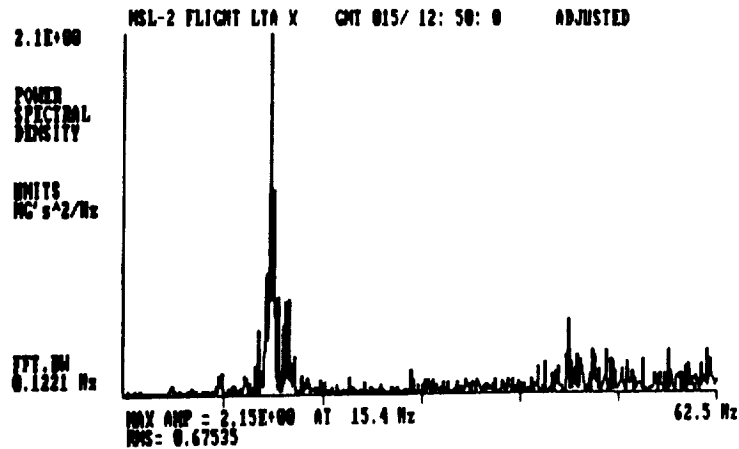


FIGURE 23. TREADMILL EXERCISE CASE, PSD

The 8-sec filter-compensated time history is difficult to interpret since it shows peaks at over twice the saturation level (Figure 24). Although possibly valid, the effects of saturated data may contribute to these apparent amplitudes. All that can be said with certainty is that the peak amplitude is greater than 0.5 mg.

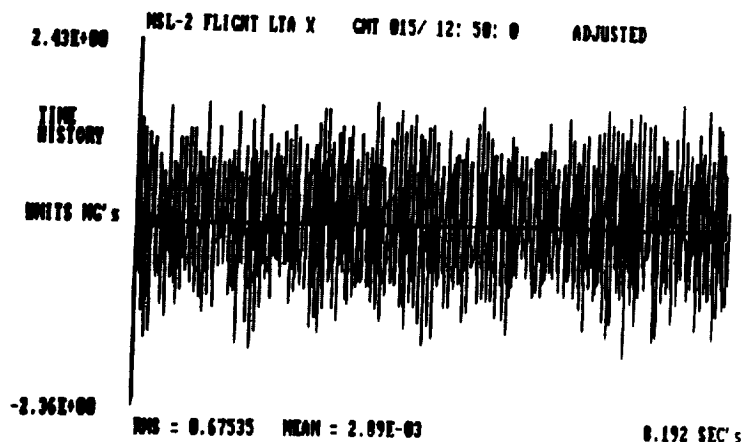


FIGURE 24. TREADMILL EXERCISE CASE, ADJUSTED

The low-frequency contribution appears small below 15.6 Hz (Figure 25). The absence of energy in the lowest portion of the spectrum appears to not justify extended low-frequency processing.

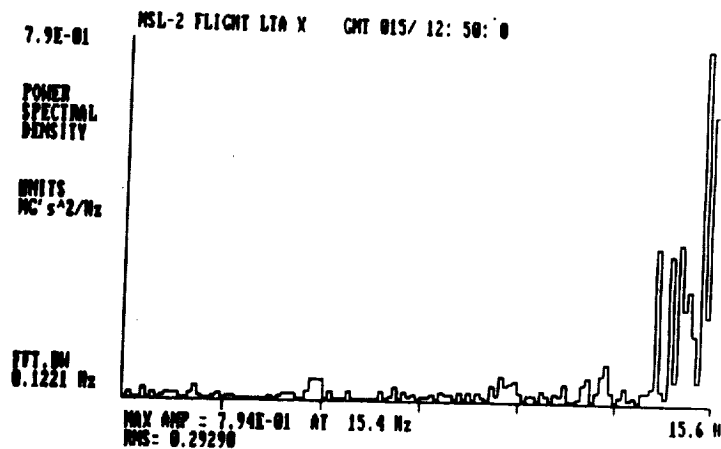


FIGURE 25. TREADMILL EXERCISE CASE, LOW-FREQUENCY PSD

Firings of the Reaction Control System (RCS) thrusters, like treadmill exercises, are intentional and occur only during crew periods of activity. X-axis accelerations are superimposed on higher frequency ringing of the structure. As with the treadmill case, a great degree of saturation occurs.

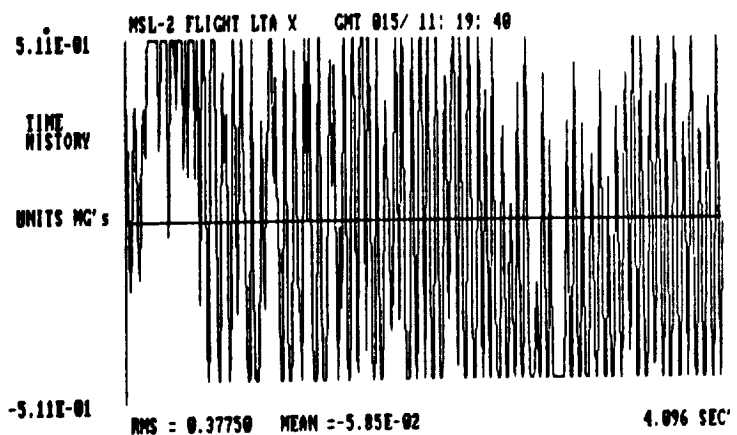


FIGURE 26. REACTION CONTROL SYSTEM, HOT FIRING, TIME HISTORY

As with the treadmill case, the apparent higher-than-saturation-level amplitudes of 2 mg (Figure 27) are possible manifestations of clipping and have not been proven valid. The actual peak amplitudes may be orders of magnitude greater.

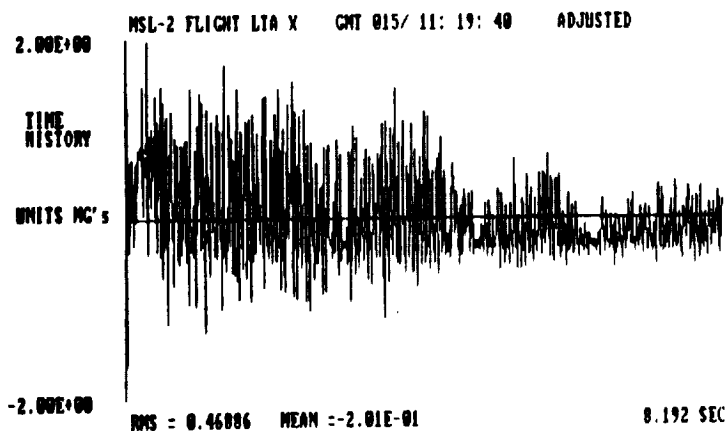


FIGURE 27. REACTION CONTROL SYSTEM, HOT FIRING, ADJUSTED TIME HISTORY

The PSD in Figure 28 shows a dominant frequency at 17.7 Hz, with a smaller contribution at low frequencies.

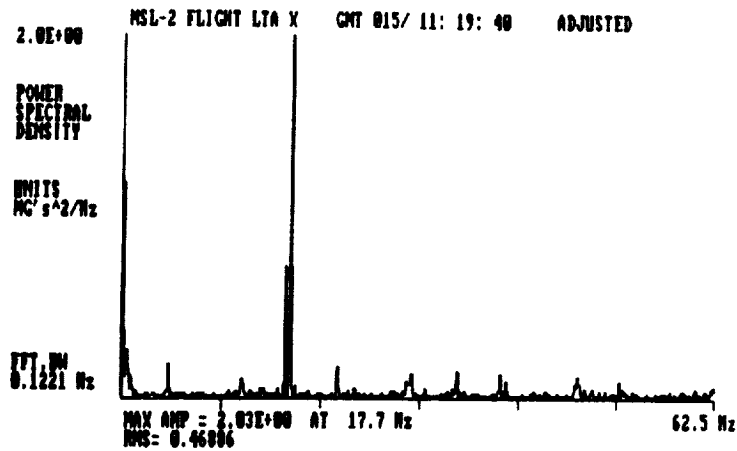


FIGURE 28. REACTION CONTROL SYSTEM, HOT FIRING, PSD

The low-frequency peak at 0.2 Hz appears significant in this case (Figure 29), with an rms amplitude of 0.13 mg. This is most likely the result of firing application rate.

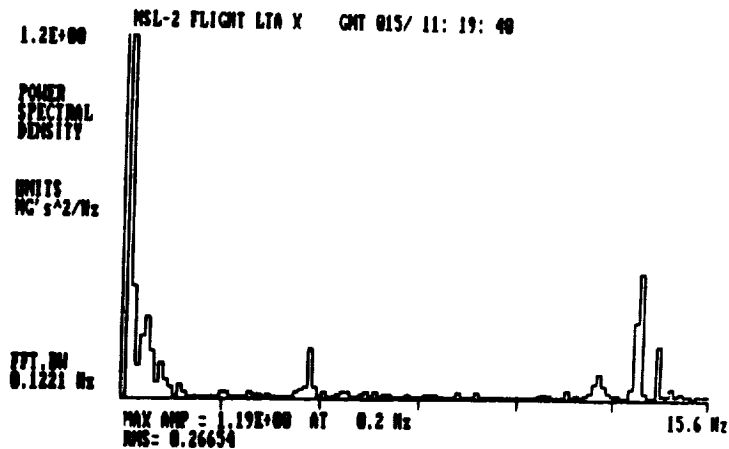


FIGURE 29. REACTION CONTROL SYSTEM, HOT FIRING, LOW-FREQUENCY PSD

The absence of crew activity does not guarantee moderate acceleration. Figure 30, taken well into the sleep period on January 15, shows a saturating acceleration during this 4-sec time history.

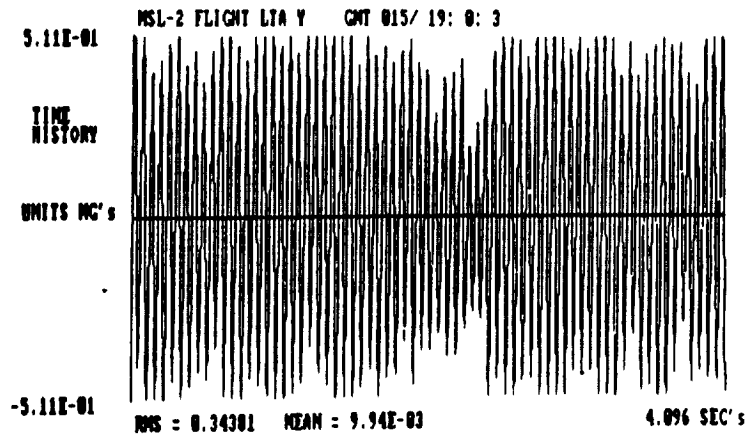


FIGURE 30. SLEEP PERIOD ON JANUARY 15, TIME HISTORY

The PSD in Figure 31 shows a highly dominant frequency of 17.1 Hz. Its cause has not yet been determined.

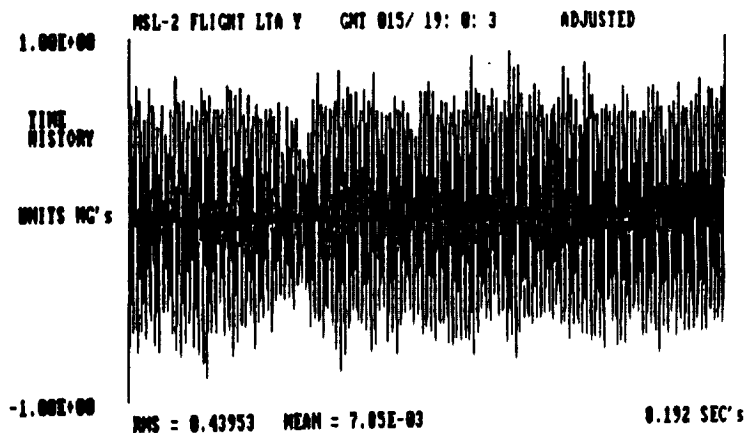


FIGURE 31. SLEEP PERIOD ON JANUARY 15, ADJUSTED TIME HISTORY

The adjusted time history (Figure 32) spans twice the period of the unadjusted time history shown before. The frequency is actually no different from that shown in Figure 30. Adjusted peaks appear to approach 1 mg.

The adjusted time history taken during a sleep period on January 17 (Figure 33) differs significantly from the January 15 case. Here, peak amplitudes do not exceed 0.2 mg over the 8-sec time span, and the total rms amplitude is 0.05 mg.

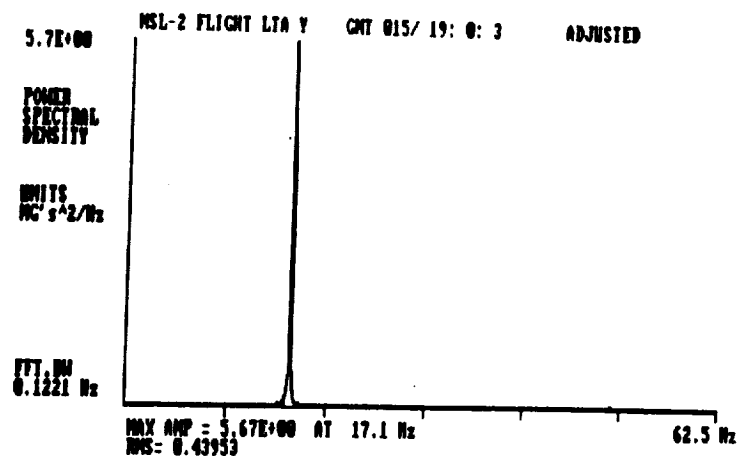


FIGURE 32. SLEEP PERIOD ON JANUARY 15, ADJUSTED PSD

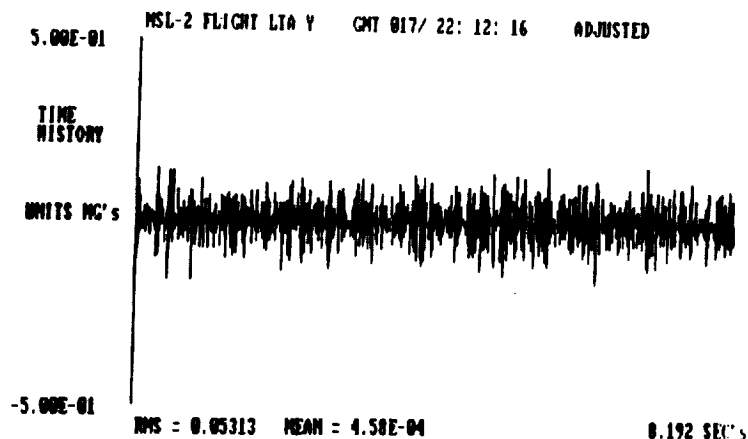


FIGURE 33. SLEEP PERIOD ON JANUARY 17, ADJUSTED TIME HISTORY

Also noticeable is the absence of a peak near 17 Hz in the PSD of the January 17 sleep case (Figure 34). The most prominent frequency of 57.4 Hz has an rms amplitude of less than 0.02 mg.

The LTA Y-axis was selected for this comparison since it exhibited greater acceleration on January 15. Both X and Z were greater than Y accelerations on January 17, with the X sensor reporting 0.1 mg RMS and the Z sensor reporting 0.011 RMS. Nevertheless, these amplitudes are significantly less in each case than those seen on January 15, and the 17-Hz component is absent in all three axes.

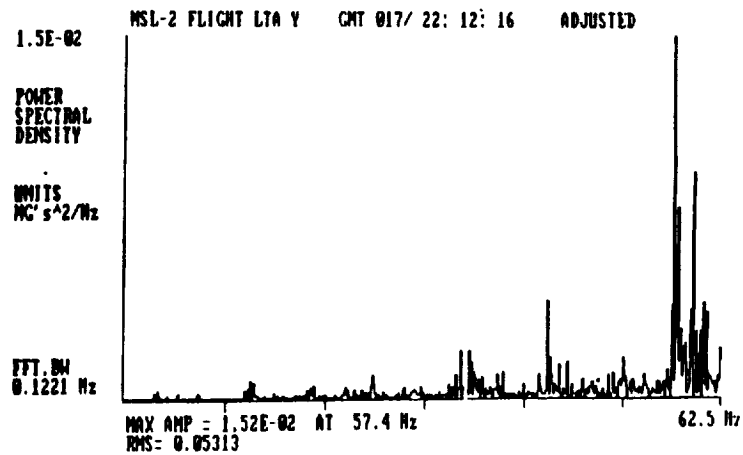


FIGURE 34. SLEEP PERIOD ON JANUARY 17, ADJUSTED PSD

The firings of vernier thrusters occur throughout the mission under control of the guidance and computer system. The IMU angle plot in Figure 35 was derived from a flight plot of yaw angular rate, and it shows the Orbiter attitude swinging between angular limits. The abrupt changes in direction are the result of firing of vernier engines located fore and aft of the Orbiter. Unless inhibited as a special operation for short periods, this activity continues throughout the mission. The case selected to show the effects of vernier firings corresponds to the first change in direction shown in this figure, during the sleep period on January 17.

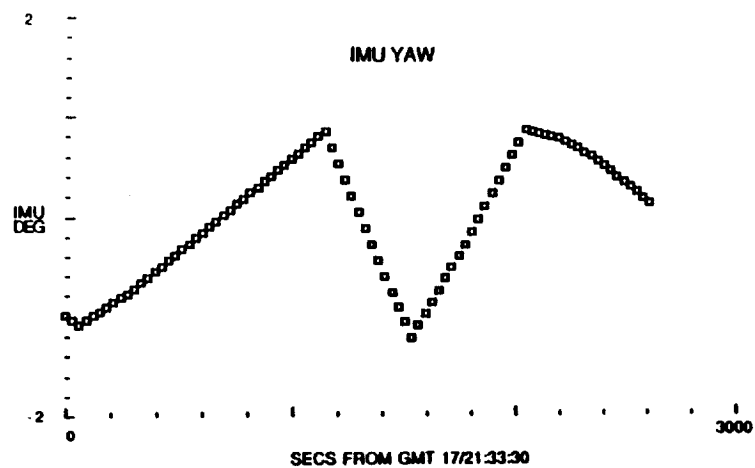


FIGURE 35. INERTIAL MEASURING UNIT (IMU) YAW, TIME HISTORY

24

Before looking at the LTA data, it is useful to examine the calculated steady-state response levels shown in Figure 36. These values, in milli-g's, have been corrected for the location of the LTA during the STS 61-C mission. Using the actual LTA location is necessary since rotational effects associated with the firings will affect the translational effects measured by the LTA. Although the combination of thrusters used for this correction may sometimes include more than the set required for pure yaw, an examination of angular position on all axes indicates no correction of rate error in pitch or roll at the same time; consequently, the plus yaw acceleration level of 0.157 mg shown here is applicable. The duration of the thruster firing required to correct the yaw rate would have been 0.3 sec.

| | \ddot{X} | \ddot{Y} | \ddot{Z} |
|---------|------------|------------|------------|
| + PITCH | -0.026 | 0.0 | -0.415 |
| - PITCH | 0.014 | 0.0 | -0.055 |
| + YAW | 0.026 | 0.157 | -0.191 |
| - YAW | -0.051 | -0.157 | -0.225 |
| + ROLL | 0.015 | 0.210 | -0.275 |
| - ROLL | -0.028 | -0.210 | -0.195 |

NOTES:

1. UNITS ARE IN MG'S.
2. DERIVED FROM ACTUAL MSL-2 LTA LOCATION AND NOMINAL ORBITER CG.
3. THRUSTER COMBINATIONS ARE TYPICAL. OTHER COMBINATIONS ARE POSSIBLE.
4. DURATION OF FIRINGS ARE MULTIPLES OF 80 msec.

FIGURE 36. LTA SENSITIVITY TO VERNIER FIRINGS

The vernier firing effect was seen predominantly by the Y-axis accelerometer as vibration (Figure 37). Structural ringing at a moderate frequency is masking the short-duration input.

The principal frequency of 17.7 Hz predominates the PSD (Figure 38). This frequency was absent before the vernier firing. It would appear that the verniers excite the same mode that was excited during the sleep period on January 15, and as commonly seen during other times of severe vibration input.

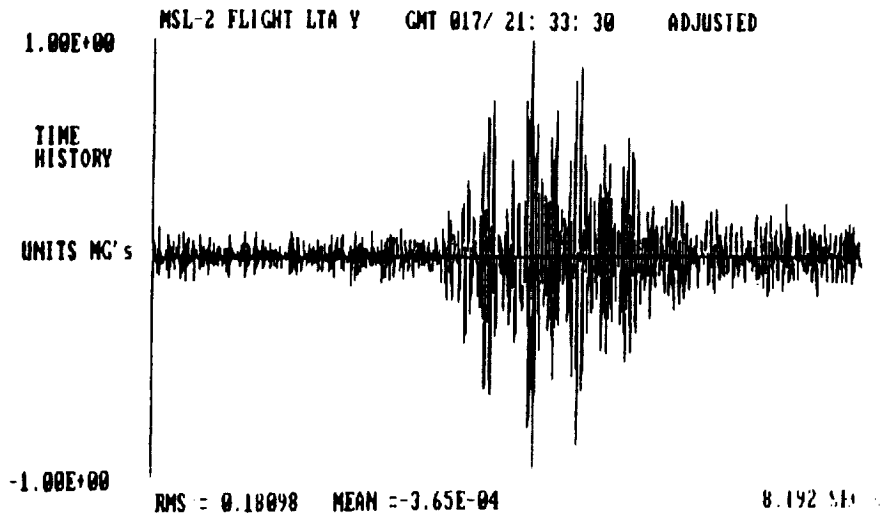


FIGURE 37. VERNIER FIRING, LTAY TIME HISTORY

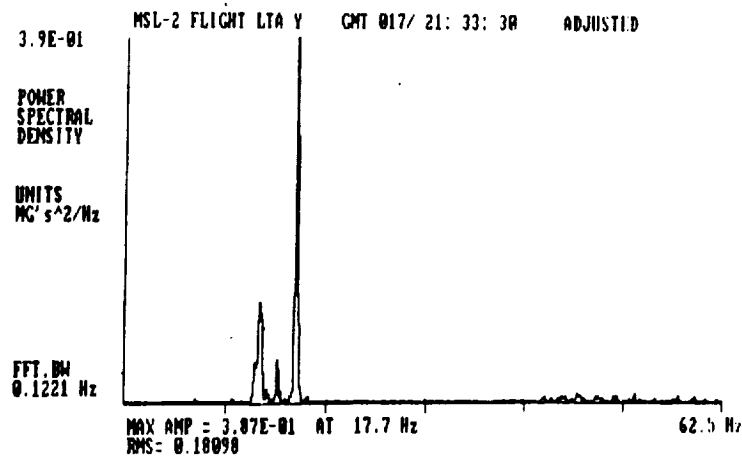


FIGURE 38. VERNIER FIRING, POWER SPECTRAL DENSITY

Other noise spikes, such as these shown in Figure 39, have no known origin. This plot shows two spikes of the same nature separated by 2 sec during the sleep period on January 12. A common occurrence, they may also occur singly or in pairs with opposing direction. There is frequently no apparent correlating activity on other axes.

Although not as spectacular as the treadmill and RCS hot fire cases shown earlier, these are possibly of more concern to acceleration-sensitive experiments since they represent an acceleration that is sustained for several tenths of a second above the 0.2-mg level.

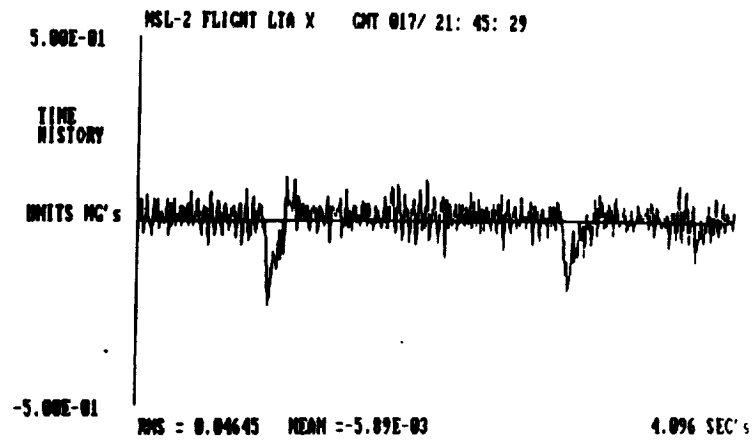


FIGURE 39. UNEXPLAINED SPIKES, TIME HISTORY

The PSD for the spike in Figure 40 shows a predominant frequency around 45 Hz. The 17-Hz source appears to not be excited.

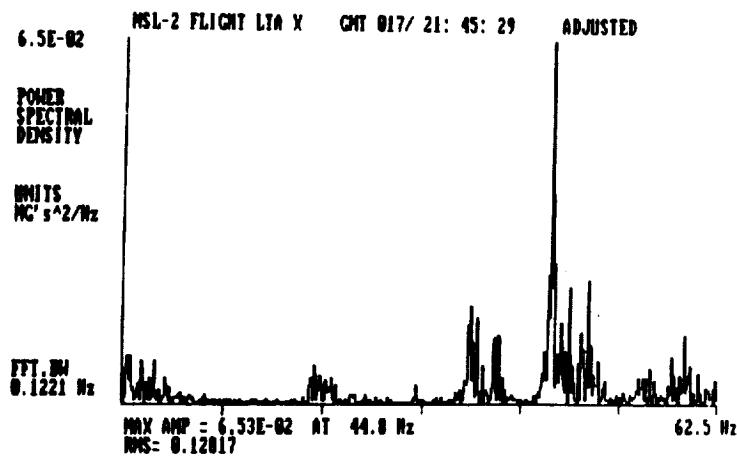


FIGURE 40. UNEXPLAINED SPIKES, PSD

Also seen during the sleep period on January 17 was this high-amplitude, short-duration burst on all three axes (Figure 41).

Figure 42 examines this burst to see its structure. It appears to begin at a higher frequency and rapidly ceases. The total duration of the burst is around 0.1 sec.

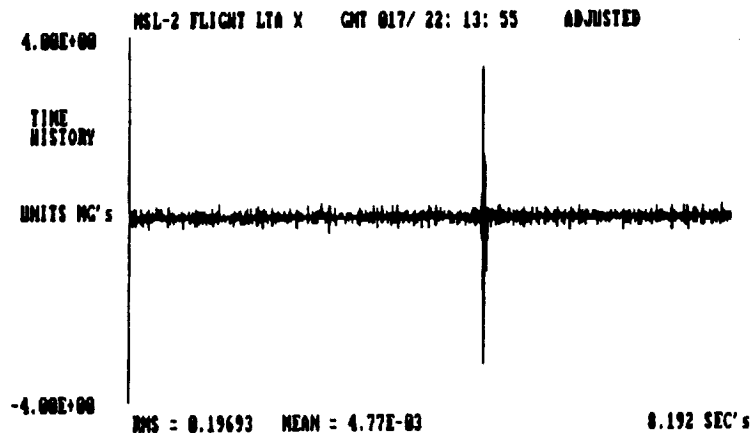


FIGURE 41. UNEXPLAINED BURSTS, TIME HISTORY

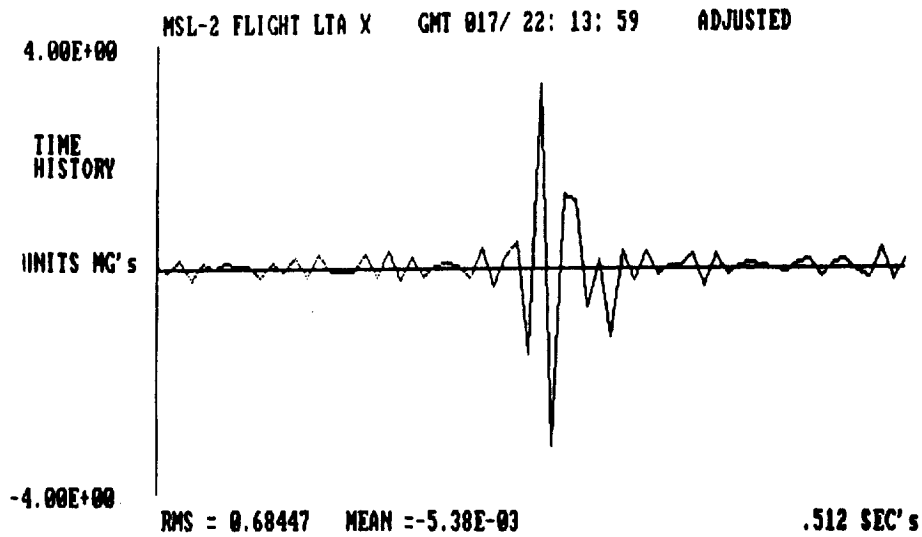


FIGURE 42. DAY 17 UNEXPLAINED BURST-EXPANDED TIME HISTORY

The PSD also indicates that no single frequency was predominant, but that the frequency range was primarily above 30 Hz (Figure 43). Possibly, the rapid stopping of rotating machinery could explain this occurrence.

To help explain the frequency of occurrence of these spikes and bursts, we examined all LTA data throughout the mission on 2-hour plots to identify periods of quiet and noise. Figure 44 is a sample of the results, which show the maximum periods of time, in minutes, between

saturations of each accelerometer axis. The first line shows that the maximum clear interval on January 17 between 17:00 and 17:30 was 2.5 min in X, 3.0 min in Y, and 3.0 min in Z. The maximum clear span of 7.5 min shown on the bottom line was duplicated several times on January 17 and 18 but was never exceeded.

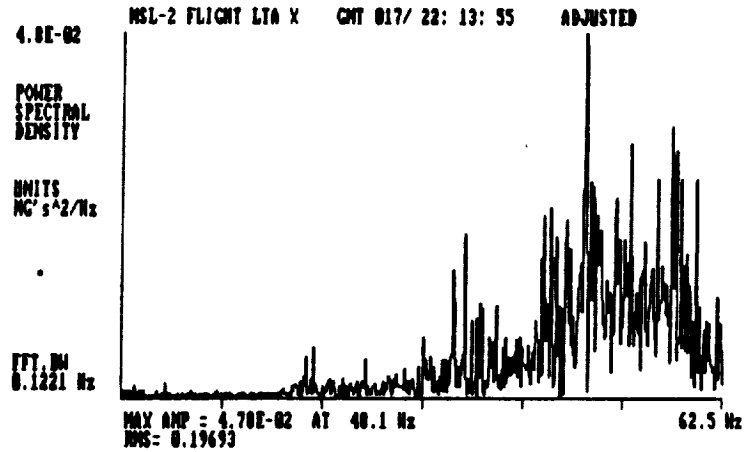


FIGURE 43. UNEXPLAINED BURSTS, PSD

| | x | y | z |
|----------|------|------|------|
| 17/17:00 | 2.5 | 3.0 | 3.0 |
| :30 | 7.5 | 8.0 | 2.0 |
| 17/18:00 | 2.5 | 4.0 | 2.0 |
| :30 | 2.5 | 3.0 | 2.0 |
| 17/19:00 | 8.0 | 4.0 | 4.0 |
| :30 | 2.5 | 7.0 | 1.0 |
| 17/20:00 | 4.0 | 2.5 | 1.5 |
| :30 | 11.0 | 12.5 | 7.5 |
| 17/21:00 | 8.0 | 5.0 | 7.0 |
| :30 | 6.0 | 15.0 | 10.0 |
| 17/22:00 | 5.0 | 2.5 | 7.5 |
| :30 | 7.0 | 7.5 | 7.5 |
| 17/23:00 | 7.0 | 6.0 | 6.0 |
| :30 | 8.0 | 8.0 | 7.5 |

FIGURE 44. MAXIMUM TIME BETWEEN SATURATIONS, GMT DAY 17

As a result of our study, we have drawn the following conclusions:

- The MSL carrier acceleration contribution is small with respect to other accelerations present on the Shuttle. We see no effect of MSL system operation in the LTA data.
- Although acceleration levels are greatly reduced in apparent severity by absence of crew activity, crew sleep periods do not ensure a quiet acceleration environment. Acceleration levels in excess of 0.5 mg occur throughout sleep periods.
- The use of gravity-gradient stabilization, which is difficult to achieve as a practical matter, will not guarantee low acceleration levels. Many 0.5-mg accelerations appear not to be connected with vernier thruster operation.

- **MSL ACCELERATION CONTRIBUTION IS SMALL WITH RESPECT TO ORBITER BACKGROUND**
- **NEITHER DAY NOR NIGHT ACTIVITIES GUARANTEE ABSENCE OF SHORT DURATION 5×10^{-4} ACCELERATION LEVELS**
- **INHIBITING VERNIER THRUSTERS WILL REDUCE BUT NOT ELIMINATE 5×10^{-4} ACCELERATION LEVELS**

FIGURE 45. CONCLUSIONS

Question: I have a question about this power spectral density. The low-frequency interface part seems to be very low and flat, whereas in a real instrument you should have showing a certain frequency. So I was just wondering whether you don't have a high-pass filter just to see the disturbances, but you just filtered off the low-frequency end.

Henderson: There is a filter in the low-frequency end, is that the question? Is there anything filtering out the low-frequency part of it? Yes, there is, but it's way beyond the range that you see there. The low-frequency cutoff is 0.01 Hz, which is well beyond the range of that PSD.

Question: So low frequency is really that quiet, then, below 10 Hz.

Henderson: What we intend to do is to really blow up one long period of time during sleep and see what does crop up because we could be missing some frequencies of 0.05, 0.07 Hz unless we go to that amount of trouble, but there is nothing observable in what we have now.

Question: You had one chart, I believe, where you said you had the sensor cut off and we were looking at electronic noise.

Henderson: Yes, the LTA was off but the Command and Data Management System (CMDS) system was on.

Question: It seems that I recall seeing 1/F noise on that chart.

Henderson: Yes. Any random noise that was present there would be amplified by our inverse filter.

Question: I realize it was there and not when the sensor was on?

Henderson: I attribute that to the fact that there was random noise present getting through the system and so it would be amplified more because of that filter. The inverse filter is amplifying by a factor of 8 to 16, so any noise that is present there would be greatly accentuated.

Ulf Merbold, ESA/ESTEC: The 17-Hz resonant frequency, is there any information why it shows up so distinctly?

Henderson: We haven't found any; someone has pointed out that it might be a submultiple of 1,000 Hz, but it doesn't seem likely to me.

Question: That is close (17 Hz) to the structural frequency of the Orbiter, a major mode of the Orbiter.

Henderson: There is a major mode at much lower frequencies. I am not aware of a resonance at 17 Hz.

